Colloids and Surfaces A: Physicochemical and Engineering Aspects 653 (2022) 129987

Contents lists available at ScienceDirect

Colloids and Surfaces A: Physicochemical and Engineering Aspects

journal homepage: www.elsevier.com/locate/colsurfa

Foamability and foam stability of oily mixtures

T. Arnaudova [a], Z. Mitrinova [a], N. Denkov [a], D. Growney [b], R. Brenda [b], S. Tcholakova [a,*]

[a] Department of Chemical Engineering, Sofia University, Sofia, Bulgaria
[b] Lubrizol Ltd, Nether Lane, Hazelwood, Derbyshire DE56 4AN, UK

GRAPHICAL ABSTRACT

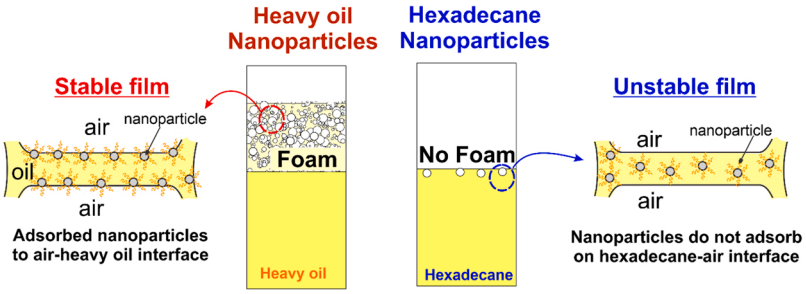

ARTICLE INFO

Keywords:
Non-aqueous foams
Mineral oils
Spreading
Oily films
Surface properties

ABSTRACT

Lubricating oils consist of base oil, containing different hydrocarbons, and modifying components (additives) which improve the application performance. Some of these additives are able to stabilize entrained air bubbles, potentially causing serious problems for engines, transmissions and hydraulic systems. Here we evaluate the foamability and foam stability of model mineral oils (hexadecane, light oil, heavy oil and their mixtures) in the presence and in the absence of nanoparticles as additives, at several temperatures. The results allow us to categorize the systems studied into three groups: (1) Oils unable to entrap any air during the stirring period; (2) Oils able to entrap air during stirring, but unable to retain it after stopping the stirring; (3) Oils which form stable bubbles and foams. Hexadecane, with and without nanoparticles, falls into the first group. Heavy oil in the presence of nanoparticles falls into the third group, whereas all other mixtures are in the second group. The inability of hexadecane to entrain air is related to its low viscosity and very low foam film stability which leads to instantaneous coalescence of the bubbles formed. The increased foamability of heavy and light oils and their mixtures is explained by: (1) their higher viscosity as compared to hexadecane which leads to slower foam film thinning and (2) the presence of long chain alkanes in these oils which create weak steric repulsion between the foam film surfaces. The addition of nanoparticles increases the foamability and the foam stability of heavy oil, without changing significantly the foam properties of the light oil and hexadecane. The latter effect is explained by the inability of the particles to attach to the light oil-air and hexadecane-air interfaces, whereas the same particles adsorb on the heavy oil-air interface and create additional steric repulsion between the air bubbles, thus allowing the formation of stable foam.

* Correspondence to: Department of Chemical and Pharmaceutical Engineering, Faculty of Chemistry and Pharmacy, Sofia University, 1 James Bourchier Ave., 1164 Sofia, Bulgaria.
E-mail address: SC@LCPE.UNI-SOFIA.BG (S. Tcholakova).

https://doi.org/10.1016/j.colsurfa.2022.129987
Received 29 May 2022; Received in revised form 5 August 2022; Accepted 15 August 2022
Available online 17 August 2022

1. Introduction

Foams are thermodynamically unstable systems in which a gas phase is dispersed in the continuous phase, which is in liquid state (liquid foams) or in solid state (solid foams). From the liquid foams, most widely studied are the aqueous foams which are commonly used or formed as byproducts in various technologies [1–3]. Non-aqueous liquid foams have started to draw the attention of researchers in recent years, due to their unwanted formation in lubricant and fuel industries, where the fluid aeration can create significant problems for the hardware (oil starvation, wear of solid surfaces, noise vibration and harshness, cooling efficiency, hydraulic pressure change and oxidation/corrosion). The prevention of air bubble incorporation in the lubricating oils requires knowledge about the mechanisms of foam stabilization and about the additives that can act as foam stabilizers. Three sources of foam stabilization have been identified for non-aqueous foams: specialty surfactants, crystalline particles, and particle adsorption at the liquid-gas interface [4,5].

The crystalline particles can adsorb on the oil-air interface and/or induce gelation in the continuous phase, thus preventing the three destabilization mechanisms for liquid foams – liquid drainage, bubble coalescence and bubble Ostwald ripening [5–7]. The change of the crystals' structure from α-solid to lamellar liquid crystalline phase leads to a significant decrease in the foam stability [8]. The increase in temperature for these systems leads to solubilization of the crystals in the oily phase and to related decrease of the foamability and foam stability [9]. The stabilization of non-aqueous foams by solid particles is often caused by adsorption of these particles onto the oil-air interface without gelation of the oily phase [10–14]. It was shown that for a given class of particles, the surface tension of the foamed oil is a crucial parameter for foam generation. For example, oily foams are formed in the presence of polytetrafluorethylene (PTFE) particles when the oil-air interfacial tension is between 30 and 45 mN/m [12]. At lower surface tension, the particles are completely wetted by the oil and do not adsorb on the oil-air interface, whereas for oils with higher surface tension powder-like materials are formed [12]. Binks et al. showed that the threshold surface tension below which the particles are completely wetted by the oils depends also on the surface chemistry of the particles. The modified particles with high fluorine content are able to stabilize the foams formed from oils with surface tension as low as 28 mN/m [14].

Conventional hydrocarbon surfactants used for aqueous foams cannot stabilize the non-aqueous foam (except for the cases when they form crystal particles in the oily phase), because they do not adsorb on the oil-air interface, due to its low interfacial tension [4,5]. On the other hand, substances based on fluorocarbons or polydimethylsiloxanes (PDMS) can adsorb on the oil-air interface, because the surface energy of fluorocarbons and PDMS is lower than that of hydrocarbons [4] and, therefore, can increase the stability of oily foam films, as shown by Bergeron et al. [15].

In recent studies by Fuller group [16,17], it was shown that non-aqueous foams can be stabilized by the so-called "evaporation-induced stabilization mechanism", which is operative when volatile liquid components generate spatial heterogeneity, which leads to Marangoni flows from the meniscus to the foam film region, thus decreasing the rate of film thinning. The foam stability is affected by the fraction of volatile components in the oily mixtures [17].

It is well known from the literature that the rheological properties of the continuous phase have a significant impact on the foam formation and stability [16–20]. For non-aqueous foams it was shown that the increase of liquid viscosity leads to a significant increase in the stability of the foams formed, due to lower rate of liquid drainage from the foam films [10]. On the other hand, the foamability of the liquids with higher viscosity is more difficult [19] and it is unclear in advance which of these factors with opposite effects would prevail in a specific system.

Most lubricating oils have complex compositions, containing a number of different performance-boosting additives, some of which are colloidally dispersed nanoparticles [20–22]. These oils routinely experience different operating temperatures which may change the properties of the additive mixtures due to a lowering of the viscosity with temperature and, in some cases, due to the evaporation of volatile base-oil components. One way to overcome these problems is to perform systematic studies with model hydrocarbons and investigate the effect of various additives on the foam properties at different temperatures.

The major aim of the current study is to clarify the mechanisms of foam generation and foam stabilization after stirring for a series of hydrocarbon fluids (hexadecane, light and heavy oil) and their mixtures (heavy oil + light oil, heavy oil + hexadecane) in the presence and absence of dispersed nanoparticles at temperatures between 25 and 80 °C. To achieve this aim, we performed foaming experiments under well-defined hydrodynamic conditions and model experiments for obtaining information for the bulk, surface and foam film properties of the studied oil mixtures.

The paper is organized as follows: in Section 2 the materials and methods are described, in Section 3 the experimental results from the foaming and model experiments are presented, in Section 4 a comparison between the mechanisms known from the literature and the mechanism proposed in the current study is made. Section 5 summarizes the main conclusions of our study.

2. Materials and methods

2.1. Materials

Three mineral oils were studied: Heavy oil (330760), Light oil (330779) and Hexadecane (H6703), all products of Sigma-Aldrich. These mineral oils were purified to remove surface-active contaminants by passing them through a glass column filled with Florisil adsorbent. Oil mixtures were prepared by mixing Heavy oil + Hexadecane and Heavy oil + Light oil in 1:1 vol ratio. The following abbreviations are used throughout the text: Heavy oil (HO), Light oil (LO), Hexadecane (HEX), Heavy oil + Hexadecane (HO+HEX) and Heavy oil + Light oil (HO+LO).

The tested additive denoted as S1 in the text is dispersion of nanoparticles in mineral oil with a mean intensity average diameter of 8.6 nm and small fraction of aggregates with size of around 200 nm. The studied nanoparticles contain a spherical metal carbonate core, sterically stabilized by alkylbenzene sulfonic acid. In other words, these particles have solid core covered by soft surfactant shell. The particles are synthesized using a multi-stage procedure and remain dispersed in the mineral oil in which they are formed. These particles are also called "overbased" detergents [21,22]. Control experiments with pure mineral oil (without particles) show that the main effects observed in our experiments come from the particles, not from the mineral oil in which they are dispersed.

The mixtures of the studied oils with S1 dispersion of nanoparticles were prepared by measuring the required amount of S1 and adding the studied oil. The final dispersion was stirred at room temperature for 20 min and sonicated using an ultrasonic bath for 20 min before the actual experiments. The samples were then stored at room temperature and remained stable for more than a year. All samples were prepared weight to weight.

2.2. Foaming method

Two shaking methods (Bartsch and Vertical shake methods) were initially tested but the studied oils and their mixtures with S1 were unable to entrap air due to the relatively high oil viscosity. To overcome this problem and to generate foam, the oil mixtures were stirred intensively using Ultra-Turrax rotor-stator device, denoted as UT in text (produced by Janke & Kunkel GmbH & Co, IKA-Labortechnik).

The foaming procedure was the following: 40 mL oil mixture was

placed in a 100 mL glass cylinder and left to equilibrate in a water bath at a given temperature for 10 min. During the entire foaming experiment, the cylinder was immersed in the water bath. The Ultra-Turrax equipped with tool S 25 N-18 G was placed inside the cylinder always at the same height (corresponding to 60 mL liquid level when the tool was immersed), ensuring similar hydrodynamic conditions in the various experiments. The foaming experiments were performed at 13,500 rpm for 5 min – the UT device was fixed while the cylinder was moved manually up and down during the foaming experiment to ensure a homogeneous stirring in the entire sample. In all cases we measured the upper level of the dispersion (liquid+bubbles) after foaming and subtracted the volume of the used oil which was 40 mL in all cases, thus determining the volume of entrapped air in the oil. Illustrative picture of one of the samples is shown in Fig. S1 in supporting information. The reproducibility in these measurements was within ± 10 %. The volume of entrapped air was measured at time intervals of 30, 60, 120, 300 s. In most cases, the bubbles formed were unstable and changed very rapidly their size as a result of bubble-bubbles coalescence. Therefore, information about the bubble size is not presented in the manuscript.

After 5 min of stirring the apparatus was stopped, the UT tool was taken out and the stability of the bubbles was monitored for additional 5 min. These experiments were performed at four temperatures: 25, 40, 60 and 80 °C.

2.3. Bulk viscosity of the formulations

The viscosities of the studied oils were measured with a rotational rheometer (Discovery Hybrid 3 Rheometer, TA Instruments). These measurements were performed with a cone-and-plate geometry (cone angle of 1° and diameter of 40 mm). Steady-shear rheological tests were applied using the following protocol: the shear rate was varied logarithmically and stepwise from 0.01 s^{-1} to 1000 s^{-1}. The dynamic viscosity was measured as a function of the shear rate. The consecutive rheological measurements were performed at four temperatures: 25, 40, 60 and 80 °C, after sample equilibration for 150 s at a given temperature.

2.4. Behavior and stability of vertical foam films

The behaviour of vertical foam films formed on a rectangular glass frame was studied using an experimental setup including a table on which a vessel filled with the investigated oil sample was positioned. Initially, a glass frame with inner area of 1 × 2 cm^2 attached to a hook was immersed in the oily solution. The foam film was formed by moving the table downwards and observed through the optical glass wall of the experimental cell with video-camera, see Fig. S2 in Supporting information. Note that the foam films formed in this method are much bigger in area as compared to the films formed between the top layer of bubbles and the atmosphere in the actual foaming experiments. Special precautions were taken to prevent the oil evaporation from the foam film surfaces during the experiment. These experiments were performed at 25 °C and 40 °C. The film lifetime was defined as the time between the start of moving the table downwards and the moment of film breakage.

2.5. Foam film formed between single bubble and the atmosphere (bubble under oil surface)

These experiments were performed after placing the oily phase on a glass plate, confined between cover glasses, see Fig. S3 in Supporting information. Then a single bubble with diameter of 1 ± 0.2 mm was ejected into the oily phase by a syringe equipped with a needle. The size of these bubbles is comparable to the initial size of the entrapped bubbles in the foaming experiments. Due to buoyancy, the bubble goes under the liquid surface and foam film of type air-oil-air was formed between the bubble and the atmosphere. This film was observed in reflected light on optical microscope Axioplan (Zeiss, Germany), equipped with a long-distance objective Zeiss Epiplan 20 × /0.40, CCD camera (Sony SSC-C370P) and H-264 Digital Video Recorder. These experiments were performed at room temperature.

2.6. Surface tension measurements

The Wilhelmy plate method was used to characterize the spreading dynamics of the S1 dispersion of particles in mineral oil on the surface of the studied oil samples. In these experiments, the surface tension was measured for given oil for 200 s at 25 °C or 40 °C using K10 tensiometer (Krüss, Germany). Afterwards, a drop of S1 dispersion was placed on the oil surface using a needle and the surface tension measurement continued for at least 500 more seconds. Typically, the total duration of the experiment was 700 s. The ability of S1 dispersion to decrease the oil surface tension was determined as the difference between the surface tension of the pure oil and the surface tension of the solution after S1 deposition on the oil surface, denoted as Δσ, see Fig. S4 in Supporting information.

2.7. Ellipsometry measurements

Ellipsometry measurements were conducted using Spectroscopic Imaging Ellipsometer – EP4 Accurion. The apparatus was equipped with an automatic focus scanner for high resolution. The scanning area was fixed to 550 × 650 μm = 0.358 mm^2 and the incident angle was 50°. In these experiments, the liquid phase was poured into a Petri dish. The measurements were conducted at 650 nm wavelength using 4-point measurement mode: 2 polarizers (at 0° and 180°), and 2 analyzers (at 0° and 180°) with 2 compensators (at −45° and +45°). After 300 s of surface observation, a drop of S1 dispersion in mineral oil was introduced on the interface and the measurement continued for additional 600 s. In these experiments, the adsorbed layer of nanoparticles from S1 dispersion was characterized by the respective phase shift between the *p*- and *s*- polirazation, δΔ, whereas the amplitude ratio variation was not significant which is typical for very thin adsorption layer [23]. These experiments were performed at 25 °C.

2.8. Measurement of the particle size via DLS

The size of the particles in S1 dispersion was measured by dynamic light scattering (DLS) on Zetasizer Nano ZS instrument (Malvern Panalytical). The reported results are averaged from at least three measurements at scattering angles of 173°. All experiments were performed at 25 °C. The S1 dispersion was diluted in hexadecane or octane down to 1 or 10 wt% for these measurements. The obtained results from these measurements are shown in Fig. S5 in Supporting information.

3. Experimental results

3.1. Foamability of oily mixtures

The volume of entrapped air, V_A, as a function of the stirring time is shown in Fig. 1A for oily mixtures without particles and in Fig. 1B in the presence of 3 wt% S1. Hexadecane is unable to entrap any air under all studied conditions (± 3 wt% S1 dispersion, at temperatures between 25 °C and 80 °C), whereas for all other oily mixtures V_A initially increases exponentially with time of stirring and levels off after that. Similar dependence was observed for the kinetics of air entrapment in Bartsch test with aqueous surfactant solutions [24,25] and the following expression is used to describe the experimental data:

$$V_A = V_{AMAX}(1 - \exp(-t/t_C)) \quad (1)$$

Here V_{AMAX} is the maximum air that can be entrapped in the foaming media and t_C is the characteristic time for air entrapment after which 63 % of this maximum air is reached. In the current study, Eq. (1) was used to describe the kinetics of foaming and to determine the values of V_{AMAX}

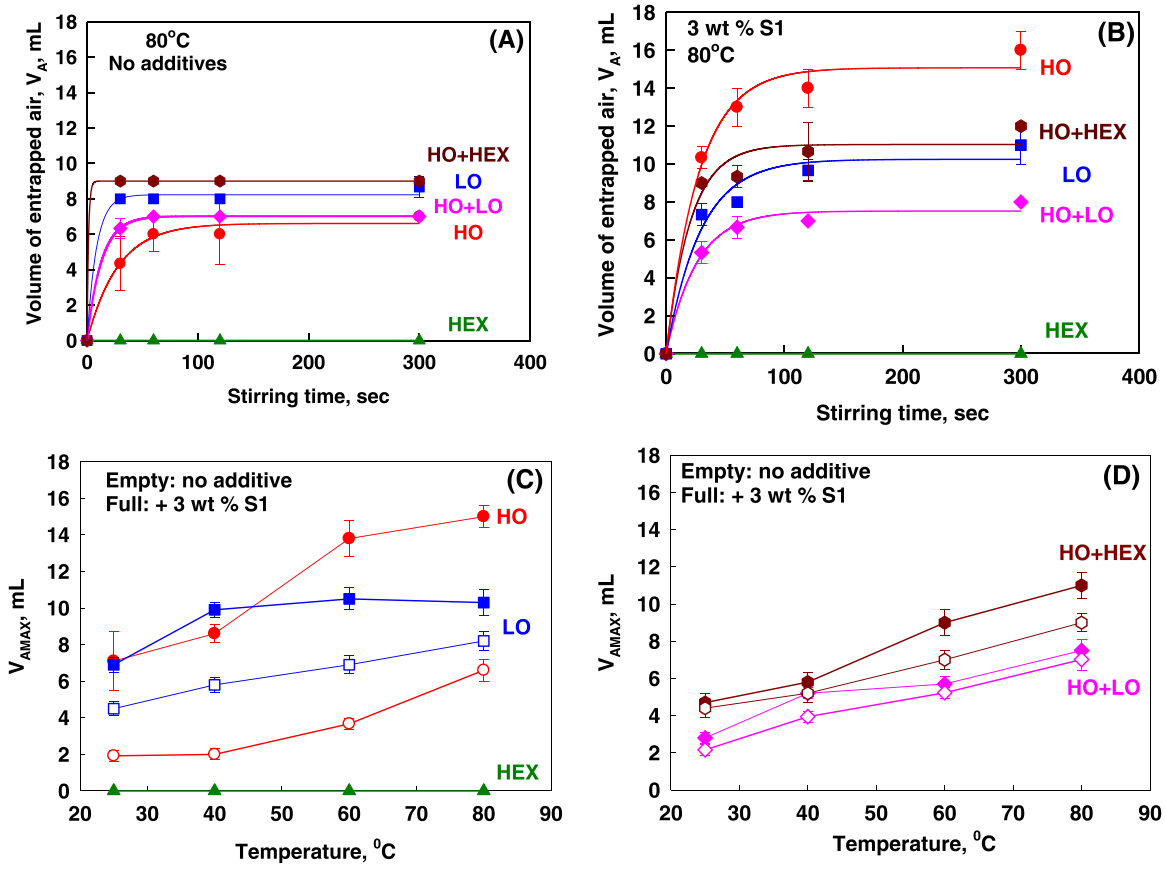

Fig. 1. (A,B) Volume of entrapped air as a function of stirring time for oily systems (A) without additives and (B) with 3 wt% S1 dispersion. The symbols are experimental data, whereas the curves are best fits according to Eq. (1). (C,D) Maximum entrapped air, V_{AMAX}, as determined from the best fit to the data as a function of temperature for hexadecane (green triangles); light oil (blue squares); heavy oil (red circles); heavy + light oil mixture (pink diamonds); and hexadecane + heavy oil mixture (dark red hexagons). (For interpretation of the references to colour in this figure legend, the reader is referred to the web version of this article.)

and t_C for the different foaming media and temperatures. The characteristic times are very short, $t_C < 20$ s and they cannot be determined precisely because the first experimental point is measured after 30 s; therefore, the values of t_C are not discussed any further, whereas the maximum volume of air, V_{AMAX} is determined precisely and the results are shown in Fig. 1C, D and S6.

An increase in temperature leads to a significant increase in V_{AMAX} for all systems studied (except for hexadecane where no air was entrapped under all conditions). The increase of V_{AMAX} with T was almost linear for HO, HO+LO and HO+HEX with and without S1, whereas a steep increase in V_{AMAX} with the increase of T from 25 °C to 40 °C was determined for LO+S1, but further increase of T from 40 °C to 80 °C had no significant impact on V_{AMAX}. The addition of 3 wt% S1 in the studied oils had a significant effect for HO, intermediate effect for LO, relatively small effect for HO+LO and HO+HEX, and no effect for HEX.

The foamability of oils without S1 is the highest for LO and HO+HEX, whereas in the presence of 3 wt% S1 at low temperatures (20 °C and 40 °C) LO and HO have similar foamability, while at high temperatures (60 °C and 80 °C) the foamability of HO+S1 is much higher as compared to that of LO+S1. The effect of S1 concentration for HO and LO is shown in Fig. S7. The foamability of LO remains almost constant up to 2 wt% S1 and increases afterwards, whereas the foamability of HO increases significantly even in the presence of 0.5 wt% S1, which is the lowest concentration investigated.

3.2. Foam stability

The typical evolution of the foam volume after stopping the stirring is shown in Fig. 2. Foams generated from solutions without additives are very unstable and all entrapped air bubbles coalesce with the atmosphere within 60 s after stopping the stirring at all temperatures. The foam stability increases significantly when 3 wt% S1 was added in the oily phase prior to stirring, see Fig. 2B. To characterize the stability of the foams formed, two characteristics were used: (1) Foam half-life time, $t_{1/2}$, defined as the time required to reach $V_{AMAX}/2$ during the storage period; (2) Percentage of retained air in the foam after 300 s of foam storage, $R_{300} = V/V_{AMAX}$. The foams for which $t_{1/2}$ is used as the main characteristic are those which are very unstable and $R_{300} = 0$, whereas the foams for which R_{300} is used are those that are rather stable and $t_{1/2} > 300$ s

The foams formed from LO, HO+HEX and HO+LO without additive have $t_{1/2} < 15$ s and all entrapped air disappears in less than 30 s. Similar behaviour was observed for foams formed from LO+S1 solutions at S1 concentration between 0.5 wt% and 3.0 wt%. Therefore, the addition of S1 to LO does not ensure stabilization of the entrapped air. The presence of 3.0 wt% S1 in HO+HEX also does not ensure stable foams and $t_{1/2} \approx 15$ s. Foams formed from HO without additive are also unstable; $t_{1/2} \approx 30$ s at all studied temperatures.

A significant increase of the stability of formed foams upon addition of S1 to HO and HO+LO solutions was observed. The dependence of R_{300} on S1 concentration at different temperatures is shown in Fig. 3. The percentage of remaining air increases from 0 to ≈ 90 % upon addition of 0.5 wt% S1 at 25 °C and 40 °C. No significant increase of R_{300} is observed upon further increase of S1 from 0.5 wt% to 3.0 wt% at these temperatures. The percentage of remaining air significantly decreases upon increasing the temperature and, as a consequence, R_{300} decreases from 90 % down to 30 % for foams formed at 60 °C and 80 °C. At these

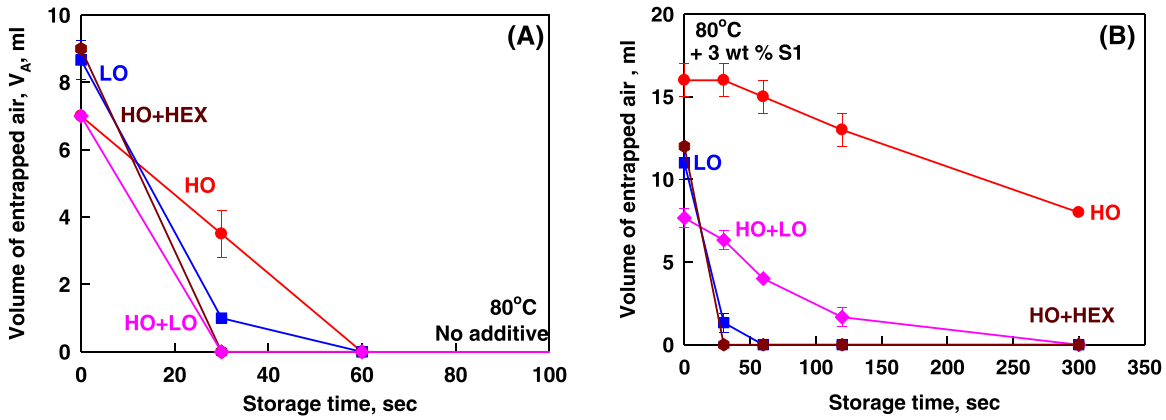

Fig. 2. Volume of entrapped air as a function of storage time after stopping the stirring for foams formed from oil systems (A) without additives and (B) in the presence of 3.0 wt% S1 dispersion of nanoparticles. The symbols are for light oil (blue squares); heavy oil (red circles); heavy + light oil mixture (pink diamonds); hexadecane + heavy oil mixture (dark red hexagons). The temperature during these experiments is 80 °C. (For interpretation of the references to colour in this figure legend, the reader is referred to the web version of this article.)

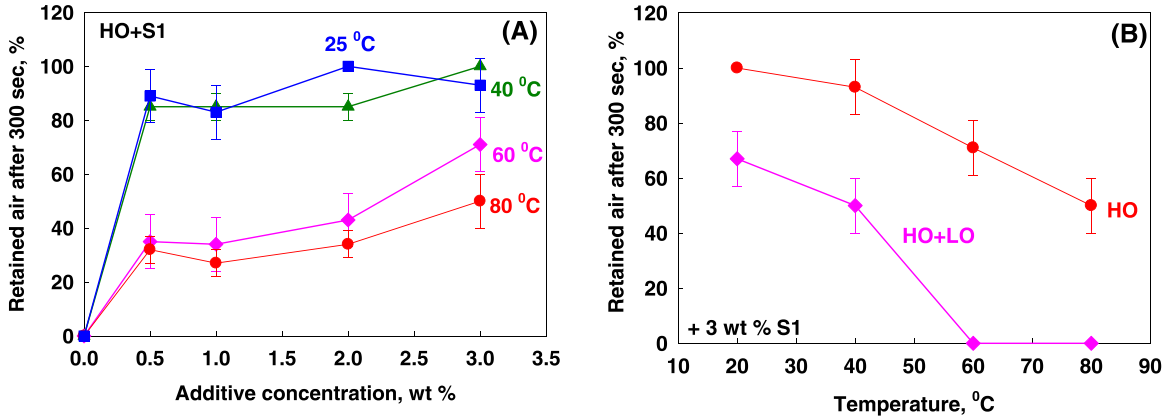

Fig. 3. Percentage of retained air after 300 s of foam storage as a function of (A) concentration of S1 particle dispersion in HO at four different temperatures and (B) Temperature for HO and HO+LO mixtures in the presence of 3 wt% S1 in the mixtures.

latter temperatures, the increase of S1 concentration leads to higher value of R_{300}. The effect of temperature on R_{300} for HO and HO+LO solutions containing 3.0 wt% S1 is shown in Fig. 3B. For both systems, R_{300} decreases with increasing the temperature. The foams formed from HO+LO are less stable as compared to those formed from HO and there is no air remaining in HO+LO when the foams are stored at 60 °C or 80 °C, even in the presence of 3.0 wt% S1.

From this series of experiments, we can conclude that: (1) HEX and its mixture with 3.0 wt% S1 is unable to entrap any air during the stirring period; (2) Light oil and HO+HEX facilitate air entrapment during stirring, but the formed foams are very unstable – the foam lifetime is < 15 s. The addition of S1 to these oils increases the amount of entrapped air, but does not affect $t_{1/2}$, which remains < 15 s (3) HO and HO+LO in the absence of S1 have intermediate capacity to entrap air and the foams formed are very unstable, $t_{1/2} \approx 30$ s for HO and $t_{1/2} \approx 15$ s for HO+LO. The addition of S1 to these oils leads to the formation of relatively stable foams at 25 °C and 40 °C which retain > 50 % of the entrapped air at 300 s after stopping the stirring. An increase in the temperature for HO containing S1 leads to a significant increase in foamability, but the percentage of remaining air after 300 s of storage decreases with temperature.

Therefore, we can consider three groups of oil systems: Group 1 (No foam): oils that cannot ensure even dynamic stabilization of the bubbles. The bubbles coalesce very rapidly with the atmosphere and no foam is formed after stirring. Hexadecane and its mixture with S1 fall into this group. Group 2 (Dynamic foams): Oils that can entrap air during stirring, but the bubbles coalesce almost instantaneously with the atmosphere after the stirring is stopped. In this group fall LO, HO, HO+HEX, HO+LO, LO+S1 and HO+HEX+S1. Group 3 (Relatively stable foams): Significant fraction of the entrapped air remains in the oil even after 300 s of storage after stopping the stirring. In this group are HO+S1 with particle concentration between 0.5 wt% and 3.0 wt% and HO+LO with 3.0 wt% S1 at T = 25 °C and 40 °C.

In the next sections we present results aimed to clarify the main factors affecting the foamability and the stability of these three groups of systems.

3.3. Role of solution viscosity for foam properties

The measured dynamic viscosities, η, as a function of temperature are shown in Fig. S8 for all studied oils and their mixtures with 3 wt% S1. The oil viscosity decreases with temperature as expected and it is not affected significantly by the presence of S1 of this relatively low concentration. These results show that the viscosity variations alone cannot explain the obtained results in the foaming experiments, because HO and HO+S1 mixtures have similar viscosity and very different foamability and foam stability, cf. Figs. 1 and 3.

In our previous study [19] we showed that the foamability of aqueous solutions in Kenwood mixer depends significantly on the viscosity of the continuous phase – the increase of the viscosity leads to lower amounts of entrapped air. To test this dependence for foams formed from non-aqueous phases, we plotted V_{AMAX} as a function of η for

the various systems studied, see Fig. S9 in Supporting information and Fig. 4. The data do not fall on a master curve, Fig. S9, but for all studied systems (except for hexadecane and its mixture with S1) V_{AMAX} decreases linearly with lgη. The change in the viscosity of the oily mixtures cannot explain the higher foamability of HO+S1 vs HO and the inability of Hexadecane to entrap air (independently of the presence of S1) while the effect of viscosity can explain the lower V_{AMAX} for HO as compared to LO obtained in the absence of S1. The experimental data for V_{AMAX} for HO and LO containing solutions (without S1) as a function of lgη fall on a master line as can be seen in Fig. 4. The following equation describes the results obtained without S1:

$$V_{AMAX} = 11.3 - 4.9 \lg \eta \quad (2)$$

The slope of the line V_{AMAX} vs. lgη is very similar for LO+S1 and HO+S1 solutions, while the maximum value of V_{AMAX} at lgη = 0 is much higher for HO+S1 and intermediate for LO+S1. These results show that the stability of the entrapped gas bubbles also has a significant impact on the final volume of entrapped air, beside the ability of the foaming device to deform the oil-air interface. Therefore, coalescence of the bubbles occurs during the period of foam generation. The mixture of HO with hexadecane shows a steeper decrease in V_{AMAX} vs lgη as compared to the other systems studied and, as a consequence, the data for HO+HEX at low temperatures (25 °C and 40 °C) deviate from the linear dependence.

We can conclude that the increase of the oil viscosity decreases the ability of the equipment to deform the oil-air interface and, as a consequence, the amount of entrapped air decreases linearly with lgη for the dynamic foams formed without additives. The addition of nanoparticles dispersion S1 increases significantly the foamability of LO and HO solutions. Note that the limit of lgη = 0 gives information about the volume of entrapped air at 1 mPa s viscosity of the oily phase. When particles stabilize the entire amount of entrapped air, this volume is 30 mL. When HO+S1 is used, the respective volume is around 25 mL which means that around 5 mL of bubbles coalesce with the upper oil surface during foaming. When systems without particles are used this value decreases to 11 mL, which means that around 19 mL of the introduced air bubbles coalesce with the atmosphere during stirring. When hexadecane is used, all 30 mL of gas bubbles coalesce and no any bubbles remain after stirring.

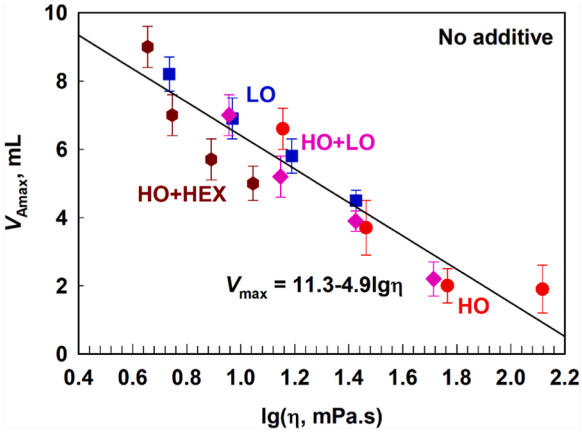

Fig. 4. Maximum entrapped air, V_{AMAX}, as a function of the logarithm of oil viscosity, lgη, for foams formed at different temperatures from LO (blue squares), HO (red circles), HO+HEX (dark red hexagons); and HO+LO (pink diamonds) without S1 particles added. The line is the best fit to all data with regression coefficient of $r^2 = 0.88$. (For interpretation of the references to colour in this figure legend, the reader is referred to the web version of this article.)

3.4. Foam films formed between single bubbles and atmosphere

The single bubbles injected in hexadecane coalesce very rapidly with the atmosphere and we cannot observe the foam films formed between the bubbles and the atmosphere. The instantaneous coalescence of the gas bubbles in hexadecane is in a very good agreement with the results from the foaming experiments where no foam was formed .

The bubbles injected in LO or HO remained stable for a certain period of time and, afterwards, coalescence with the atmosphere was observed. The typical evolution of these films is shown in Fig. S10. The films are with irregular thickness and typically break after the formation of a black (thin) spot. We measured the lifetime of the bubbles with film diameter between 100 and 200 μm. The percentage of the bubbles able to survive up to a certain time is shown in Fig. 5. The stability of the bubbles formed in LO and LO+S1 systems is much lower as compared to the stability of the bubbles formed in HO and HO+S1. At least partially the higher stability of the bubbles formed in HO is related to its higher viscosity and slower rate of film thinning when compared to LO, while the difference in the stability of the bubbles formed in HO+S1 system could not be explained by changed viscosity only. Note that the addition of S1 to LO affects only slightly the bubble stability which is also in a good agreement with the results from the foaming experiments. From this series of experiments, we can conclude that the addition of S1 to HO increases the stability of foam films, whereas its addition to LO affects only slightly the foam film stability .

3.5. Stability of vertical foam films

The stability of the vertical foam films at 25 °C and 40 °C was also studied. The typical thinning pattern of these films is illustrated in Fig. S11. Illustrative images of foam films formed from HO and HO+S1 systems are shown in Fig. 6. The film thinning was regular for the films without particles and irregular for the films from HO+S1 which shows that particle aggregates are attached to the foam film surfaces in the latter system. The thickness of the foam film formed from HO liquid was ≈ 100 nm (foam films appear white) due to the action of long-range weak steric repulsion, arising from the presence of hydrocarbon molecules with different chain lengths in the oily mixture. The probability for film rupture is shown in Fig. 7. As a characteristic for the film lifetime we used t_{50} which is defined as the time required for rupture of 50 % of the observed foam films. The films formed from HO without S1 are unstable at both temperatures (25 °C and 40 °C) and $t_{50} < 10$ s

The addition of 3.0 wt% S1 to HO leads to a significant increase of t_{50}

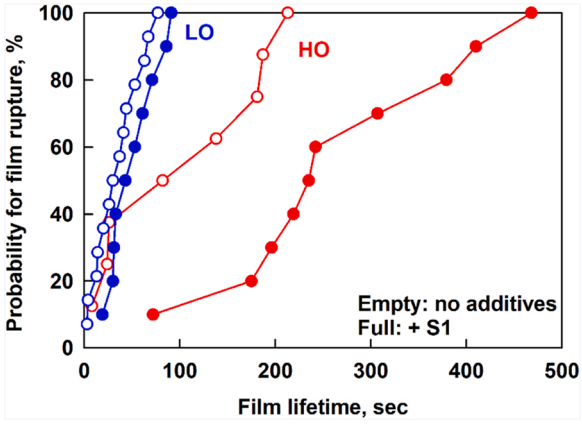

Fig. 5. Probability for film rupture for bubbles injected in LO (blue symbols) and HO (red symbols) in the presence of 3 wt% S1 (full symbols) and without S1 (empty symbols). The diameter of films formed between the bubble and atmosphere is between 100 and 200 μm. (For interpretation of the references to colour in this figure legend, the reader is referred to the web version of this article.)

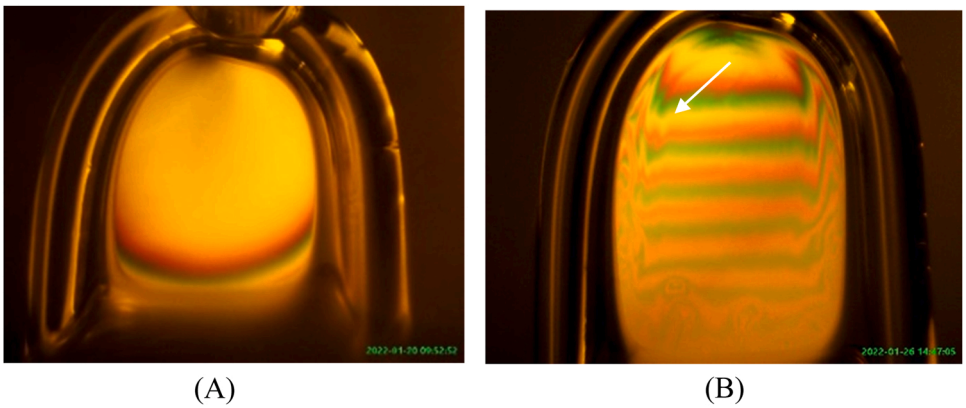

Fig. 6. Illustrative images of vertical foam films formed from (A) HO and (B) HO+ 3 wt% S1 at 25 °C. The arrow in (B) indicates one of the places where aggregates of particles in S1 affect the interference pattern between the foam film surfaces.

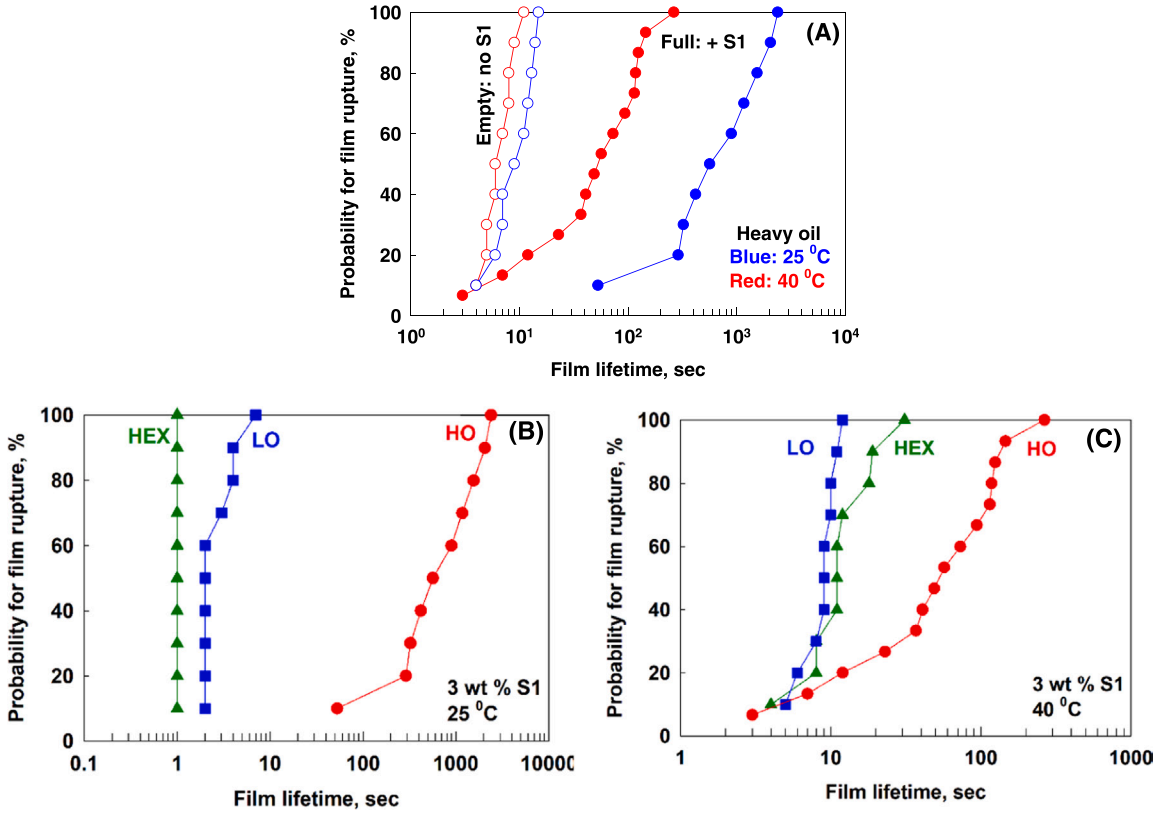

Fig. 7. (A) The probability for rupture of the vertical films formed from HO (empty symbols) and from HO+ 3 wt% S1 (full symbols) at 25 °C (blue symbols) and 40 °C (red symbols). (B,C) The probability for rupture of the vertical films formed from hexadecane (green triangles), LO (blue squares) and HO (red circles) at (B) 25 °C and (C) 40 °C. (For interpretation of the references to colour in this figure legend, the reader is referred to the web version of this article.)

to 60 s for films formed at 40 °C and to 600 s for films formed at 25 °C. This higher stability in the presence of S1 is related to the additional steric repulsion between film surfaces, arising from the adsorbed particles on the film surfaces which decelerate the film thinning, see Fig. 6B. The increase in temperature decreases the probability for particle adsorption onto the film surfaces and decreases the stability of the respective films. The stability of films formed from LO, HEX, HO+LO and HO+HEX in the presence of 3.0 wt% S1 was very low and no adsorbed particles on film surfaces were seen, see the images in Fig. S11. The stability of films from HEX+S1 at 40 °C was also low, but the films did not rupture instantaneously as it was the case at 25 °C. The higher stability at 40 °C is related to the irregular film thinning as can be seen from the images in Fig. S11. This irregularity is likely related to Marangoni effects as reported by Suja et al. [16]. Note, however, that this effect did not change the foam properties in our foaming test. At both temperatures 25 °C and 40 °C, hexadecane was unable to entrap any air in the used foaming method.

From this series of experiments, we can conclude that the foam films formed between single bubbles and atmosphere are very unstable and rupture instantaneously after their formation when hexadecane is used as oily phase without particles. Foam films formed from LO, HO and LO+S1 have higher stability as compared to those from hexadecane which is partly related to the higher viscosities of these oils and to the presence of molecules with different chain lengths which create some steric repulsion between the foam film surfaces. The addition of particles to HO strongly increases the film stability – these films become very

stable, especially at 25 °C, due to the particle adsorption onto the film surfaces. These particles create additional steric repulsion and decelerate the rate of film thinning.

Thus we conclude that hexadecane is unable to retain any air after stirring because all bubbles coalesce instantaneously with the atmosphere. The oils that retain air during stirring demonstrate dynamic bubble stabilization and, as a consequence, the volume of entrapped air increases when the decrease of oil viscosity. The addition of S1 to HO leads to particle adsorption onto the film surfaces. The adsorbed particles induce stronger steric repulsion between the foam film surfaces and strongly increase the film stability. In the latter systems, more than 90 % of the entrapped air remains after 300 s of foam storage after stopping the stirring. The temperature increase decreases the probability for particle adsorption in these systems and decreases the foam stability. Therefore, we studied also the reasons for the different particle adsorption on hexadecane-air; LO-air and HO-air interfaces.

3.6. Surface properties

The effect of particles from S1 on oil surface properties was studied by two complementary methods – surface tension measurements and ellipsometry. The experimental results from these measurements are shown in Fig. 8. The spreading of S1 over HO-air interface leads to ≈ 0.6 mN/m decrease in the surface tension and a significant change in the phase angle Δ in ellipsometry. These results prove that particles from S1 adsorb on the HO-air interface. Note that the particles are dispersed in the mineral oil in which they are initially synthesized. The dispersing oil itself has no impact on the particle spreading (checked by performing control experiments without particles). The spreading particles cover the entire surface area of the oil substrate, because we placed the drop of S1 suspension far away from the Wilhelmy plate used to measure the surface tension.

All these results are in very good agreement with the results obtained with vertical foam films where the presence of attached particles was deduced from the irregularities in the interference pattern observed in reflected light. The deposition of S1 over oil surface also leads to a decrease in surface tension for HO+LO and HO+HEX, but the effect is much smaller (as compared to HO) and close to the experimental accuracy. The deposition of S1 on LO-air and hexadecane-air interfaces did not change their surface tensions and had no impact on the measured phase angle in the ellipsometry measurements. From this series of experiments, we conclude that particles from S1 adsorb only on the HO-air interface. There is a threshold value of surface tension below which the particles are unable to adsorb the oil-air interface and this value is around the surface tension of LO, σ ≈ 28.5 mN/m. Such behaviour has been already observed in the literature for other types of particles [12].

4. Discussion

The obtained results clearly show that the foamability and the foam stability depend on both the viscosity of the continuous phase and on the foam film stability. The amount of entrapped air depends mostly on two processes which act in opposite directions: (1) The deformability of the oil-air interface which defines how easily the air bubbles can be formed and (2) The coalescence stability of the entrapped bubbles with the large oil-air interface.

The used foaming method was unable to incorporate gas bubbles in hexadecane and its mixture with particles from S1, independently of the low oil viscosity. The films formed between the gas bubbles and the atmosphere broke instantaneously. The low stability of hexadecane films when compared to those formed from LO and HO is partially due to the lower viscosity of hexadecane which leads to faster film thinning to the critical film thickness at which the foam films rupture. It is also related to the absence of any repulsive forces that can oppose the van der Waals attraction between the foam film surfaces. The latter effect is linked to the presence of only one type of molecules in hexadecane which is a pure substance. On the other hand, LO and HO contain molecules of different lengths and some of these molecules create weak steric repulsion between the foam film surfaces. The combination of higher oil viscosity and weak steric repulsion leads to the observed higher ability for these oils to retain air bubbles during the stirring period. However, after stopping the stirring, almost instantaneous bubble coalescence is observed in the absence of particles. The higher viscosity of HO increases the lifetime of the foams from 15 to 30 s, but after 60 s all bubbles disappear from the HO liquid. The calculations show that the time required for the bubbles to float from the bottom of the cylinder to its top is ≈ 30 s for 1 mm sized bubbles introduced in HO at 20 °C, whereas this time is ≈ 6 s for LO. Therefore, the weak steric repulsion in LO and HO can ensure only dynamic stabilization of these foams for a short period of time.

It should be mentioned that the mixtures of HO+HEX and LO+HO are able to incorporate some air during stirring, but the formed foams are very unstable after stopping the stirring. The higher oil viscosity leads to more difficult deformation of the large oil-air interface and lower amount of entrapped air bubbles (at given coalescence stability). That is why the amount of entrapped air decreases with increasing the oil viscosity – as a consequence the entrapped air in LO is more than that in HO (Fig. 1C). When the stirring stops, the process of bubble entrapment is ceased and the amount of retained air is governed by the coalescence stability of the bubbles. During this second (storage) stage, the foam formed in LO is less stable than that in HO, Fig. 2A, which is in a very good agreement with the results shown in Fig. 5. These explanations agree also with the results reported by Tran et al. [27] where it was shown that the non-linear variations of the surface tension of oily

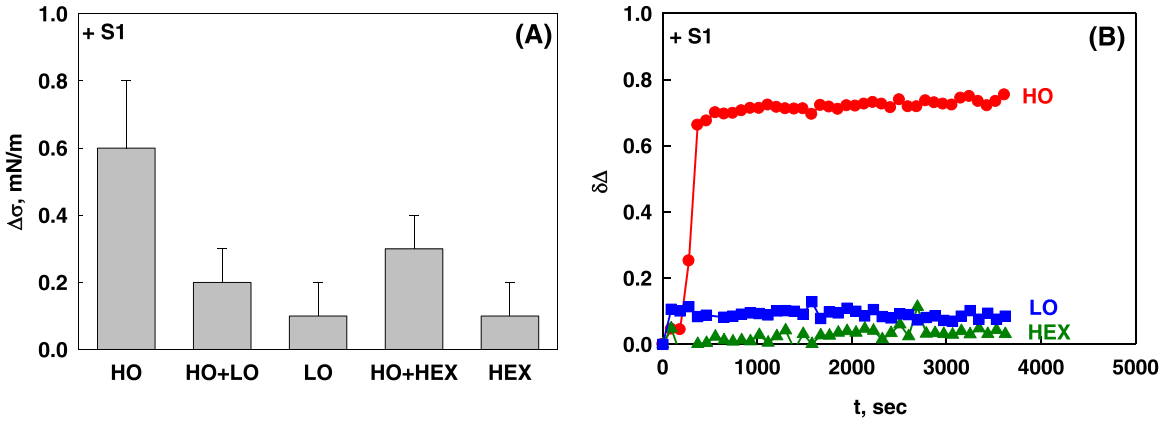

Fig. 8. The changes of (A) surface tension as measured by Wilhelmy plate method and (B) phase angle Δ measured by ellipsometry after spreading of suspension of nanoparticles S1 on different oily substrates.

mixtures can increase their foamability and the stability of the respective foam films.

The addition of S1 to different oils has a noticeable effect only for HO and HO+LO. For all other oils the presence of S1 does not affect the surface properties, does not change the stability of the respective foam films and has no effect on the foam properties. The effect of S1 on the properties of HO and a HO+LO mixture is explained with the adsorption of particles onto the HO-air interface which creates steric repulsion between the film surfaces and decelerates the rate of film thinning. The driving force for the adsorption of these particles on the air-oil interface is the presence of surfactant tails which cover the metal carbonate core of the particles. These surfactant tails are shorter as compared to the oil molecules in the medium, thus forming particles with lower surface tension as compared to that of the HO phase. Due to the lower surface tension of the particles, the latter spontaneously adsorb on the HO-air interface.

The fact that particles from S1 adsorb only on the HO-air surface is in a good agreement with the results reported in literature that particles with a given hydrophobicity attach easier to interfaces for which the oil-air surface tension is higher [14]. The measurements using Wilhelmy plate method showed that the surface tension of HO is the highest, $\sigma \approx 30.3$ mN/m, as compared to all other oils studied. The surface tension of LO is $\sigma \approx 28.5$ mN/m and the particles do not adsorb on LO-air interface. It is known in the literature that an increase in temperature decreases the surface tension of oils [26]. Indeed, the increase of temperature from 25 to 40 °C for HO leads to decrease of its surface tension from 31 to 30.3 mN/m, whereas for LO it decreases from 29.7 to 28.9 mN/m. As a consequence, the ability of the particles to adsorb on the oil-air interface decreases and the stability of formed foams also decreases with the increase of temperature, see Fig. 3. The decrease in foam stability is bigger for the HO+LO mixture, because the surface tension of this mixture is lower when compared to HO and the particle adsorption is also lower.

The hypothesis that the higher stabilization of HO and LO foams could be related to the evaporation of some volatile substances in these molecular mixtures was checked. This effect could lead to local inhomogeneities in the adsorption layers and could oppose the liquid drainage from the foam films [16,17]. We measured the evaporation rate of the studied oils at different temperatures and performed experiments with open (allowing oil evaporation) and closed cells (no evaporation). The results showed a negligible evaporation of HO and LO components (less than 0.03 % and 0.02 %, respectively, at both 40 and 80 °C) which means that evaporation-induced Marangoni effect is not expected for these oils. On the other hand, significant evaporation of Hexadecane was detected (0.4 % at 40 °C and 8.9 % at 80 °C) while the respective foams remain very unstable. The foamability of the HO+HEX mixtures was also very low and the respective foams were unstable. These results indicate that the Marangoni effects were probably of negligible significance in the systems studied.

5. Conclusions

The foamability and foam stability of different mineral oils and their mixtures were studied. Hexadecane was unable to stabilize foams during intensive stirring, due to the instantaneous coalescence of the formed bubbles with the atmosphere above the oil. The lack of any repulsion between the foam film surfaces (only van der Waals attraction in this system) leads to very unstable and short-living foam films. The studied particles did not adsorb on the hexadecane-air interface due to the lower surface tension of hexadecane. Therefore, the S1 particles had no significant impact on the foamability and foam stability for hexadecane.

In contrast, light oil and heavy oil contain saturated hydrocarbon molecules with different chain-lengths which ensure weak steric repulsion between the foam film surfaces. This steric repulsion slows down the foam film thinning and facilitates the air entrapment during stirring. On the other hand, these steric forces are insufficient to prevent the bubble-atmosphere coalescence during the resting stage. For systems with weak steric repulsion, the maximum amount of the entrapped air decreased linearly with the logarithm of oil viscosity. The temperature increase in these systems decreases the oil viscosity and increases the foamability, while it has no significant impact on the stability of the foams formed.

The particles adsorb on the HO-air interface and induce additional and stronger steric repulsion which increases significantly the foamability and the stability of the foams formed. The temperature increase in this system leads to higher foamability (due to the lower oil viscosity), while the fraction of the retained air during storage decreases, due to the suppressed particle adsorption on the HO-air interface.

Due to the lower surface tensions of light oil and hexadecane, the particles do not adsorb on the oil surface and, as a consequence, the addition of particles to these oils had no significant impact on both the foamability and the foam stability.

The obtained results and the formulated conclusions could be used as a solid basis for analysis of experimental data with similar oil-particle systems, as well as for the rational design of such systems with desired high or low (as required) foamability and foam stability.

CRediT authorship contribution statement

Turkyan Arnaudova: Investigation. **Zlatina Mitrinova:** Investigation, Formal analysis, Visualization, Writing – original draft. **David Growney:** Conceptualization, Methodology, Writing – review & editing. **Richard Brenda:** Conceptualization, Methodology, Writing – review & editing. **Slavka Tcholakova:** Conceptualization, Methodology, Formal analysis, Visualization, Writing – review & editing, Supervision.

Declaration of Competing Interest

The authors declare that they have no known competing financial interests or personal relationships that could have appeared to influence the work reported in this paper.

Data Availability

Data will be made available on request.

Acknowledgements

The authors are grateful to Dr. Nadya Politova and Dr. Sonya Tsibranska for useful discussions, and to Mr. Vassil Georgiev and Mr. Yohan Georgiev for performing some of the foaming experiments. This work was supported by Lubrizol and partially supported by the Operational Program “Science and Education for Smart Growth” 2014–2020, co-financed by European Union through the European Structural and Investment Funds, grant number BG05M2OP001-1.002-0023.

Appendix A. Supporting information

Supplementary data associated with this article can be found in the online version at doi:10.1016/j.colsurfa.2022.129987.

References

[1] R.J. Pugh, Foaming, foam films, antifoaming and defoaming, Adv. Colloid Interface Sci. 64 (1996) 67–142.
[2] D.L. Weaire, S. Hutzler, The Physics of Foams, Oxford University Press, Oxford, 2001.
[3] I. Cantat, S. Cohen-Addad, F. Elias, F. Graner, R. Höhler, O. Pitois, et al., Foams: Structure and Dynamics, Oxford University Press, Oxford, 2013.
[4] C. Blázquez, E. Emond, S. Schneider, C. Dalmazzone, V. Bergeron, Non-aqueous and crude oil foams, Oil Gas Sci. Technol.–Revue d'IFP Energ. Nouv. 69 (2014) 467–479.

[5] A.-L. Fameau, A. Saint-Jalmes, Non-aqueous foams: current understanding on the formation and stability mechanisms, Adv. Colloid Interface Sci. 247 (2017) 454–464.
[6] S.E. Friberg, Foams from non-aqueous systems, Curr. Opin. Colloid Interface Sci. 15 (2010) 359–364.
[7] M. Brun, M. Delample, E. Harte, S. Lecomte, F. Leal-Calderon, Stabilization of air bubbles in oil by surfactant crystals: a route to produce air-in-oil foams and air-in-oil-in water emulsions, Food Res. Int. 67 (2015) 366–375.
[8] R.G. Shrestha, L.K. Shrestha, C. Solans, C. Gonzalez, K. Aramaki, Nonaqueous foam with outstanding stability in diglycerol monomyristate/olive oil system, Colloids Surf. A: Physicochem. Eng. Asp. 353 (2010) 157–165.
[9] A.-L. Fameau, S. Lam, A. Arnould, Cd Gaillard, O.D. Velev, A. Saint-Jalmes, Smart nonaqueous foams from lipid-based oleogel, Langmuir 31 (2015) 13501–13510.
[10] B.P. Binks, C.A. Davies, P.D.I. Fletcher, E.L. Sharp, Non-aqueous foams in lubricating oil systems, Colloids Surf. A: Physicochem. Eng. Asp. 360 (2010) 198–204.
[11] B.P. Binks, B. Vishal, Particle-stabilized oil foams, Adv. Colloid Interface Sci. 291 (2021), 102404.
[12] B.P. Binks, A. Rocher, Stabilisation of liquid–air surfaces by particles of low surface energy, Phys. Chem. Chem. Phys. 12 (2010) 9169–9171.
[13] B.P. Binks, A. Rocher, M. Kirkland, Oil foams stabilised solely by particles, Soft Matter 7 (2011) 1800.
[14] B.P. Binks, A.T. Tyowua, Influence of the degree of fluorination on the behaviour of silica particles at air–oil surfaces, Soft Matter 9 (2013) 834–845.
[15] V. Bergeron, J.E. Hanssen, F.N. Shoghl, Thin-film forces in hydrocarbon foam films and their application to gas-blocking foams in enhanced oil recovery, Colloids Surf. A: Physicochem. Eng. Asp. 123–124 (1997) 609–622.
[16] V.C. Suja, A. Kar, W. Cates, S. Remmert, P. Savage, G. Fuller, Evaporation-induced foam stabilization in lubricating oils, Proc. Natl. Acad. Sci. USA 115 (2018) 7919–7924.
[17] S.G.K. Calhoun, V. Chandran Suja, G.G. Fuller, Foaming and antifoaming in non-aqueous liquids, Curr. Opin. Colloid Interface Sci. 57 (2022), 101558.
[18] J. Wang, Y. Yuan, L. Zhang, R. Wang, The influence of viscosity on stability of foamy oil in the process of heavy oil solution gas drive, J. Pet. Sci. Eng. 66 (2009) 69–74.
[19] N. Politova, S. Tcholakova, Zh Valkova, K. Golemanov, N.D. Denkov, Self-regulation of foam volume and bubble size during foaming via shear mixinge, Colloids Surf. A 539 (2018) 18–28.
[20] C. Callaghan, Non-aqueous foams: a study of crude oil foam stability, Foam: Phys. Chem. Struct. (1989) 89–104.
[21] D. Growney, K. Trickett, G. Walker, M. Robin, Acid neutralization rates—why total base number doesn't tell the whole story: understanding how the colloidal structure of overbased detergents influences acid neutralization rates, SAE Int. J. Fuels Lubr. 14 (1) (2021).
[22] D. Growney, K. Trickett, M. Robin, S. Rogers, D. McDowall, E. Moscrop, Acid neutralization rates—why total base number doesn't tell the whole story: understanding the neutralization of organic acid in engine oils, SAE Int. J. Fuels Lubr. 14 (3) (2021).
[23] S.C. Russev, T.V. Arguirov, T.D. Gurkov, β-Casein adsorption kinetics on air–water and oil–water interfaces studied by ellipsometry, Colloids Surf. B: Biointerfaces 19 (2000) 89–100.
[24] B. Petkova, S. Tcholakova, N. Denkov, Foamability of surfactant solutions: interplay between adsorption and hydrodynamic conditions, Colloids Surf. A 626 (2021), 127009.
[25] B. Petkova, S. Tcholakova, M. Chenkova, K. Golemanov, N. Denkov, D. Thorley, S. Stoyanov, Foamability of aqueous solutions: role of surfactant type and concentration, Adv. Colloid Interface Sci. 276 (2020), 102084.
[26] Adamson, A.W.,Gast, A.P., Physical Chemistry of Surfaces, 6th Edition, 1997.
[27] H.-P. Tran, M. Arangalage, L. Jørgensen, N. Passade-Boupat, F. Lequeux, L. Talini, Phys. Rev. Lett. 125 (2020), 178002.